Key Engineering Materials *Online: 2013-07-31*
ISSN: 1662-9795, Vols. 569-570, pp 103-110
doi:10.4028/www.scientific.net/KEM.569-570.103

Investigation of Dynamic Fracture Behavior of Graphite

Lorenzo Peroni[1,a], Martina Scapin[1,b], Federico Carra[2,c] and Nicola Mariani[2,d]

[1]Department of Mechanical and Aerospace Engineering, Politecnico di Torino

Corso Duca degli Abruzzi 24, 10129 Turin, Italy

[2]Engineering Department, Mechanical & Materials Group, CERN

1211 Geneva 23, Swizerland

[a]lorenzo.peroni@polito.it , [b]martina.scapin@polito.it , [c]federico.carra@cern.ch, [d]nicola.mariani@cern.ch

Keywords: dynamic tensile strength, spalling test, graphite, Split Hopkinson Pressure Bar.

Abstract. The strain-rate sensitivity of brittle materials, such as glass, ceramics or concrete-like materials, is usually easier to be performed in compression. However, also the tensile behavior, which affects phenomena such as spalling, scabbing and fragmentation, has to be investigated to achieve an exhaustive characterization.

In this work, the spalling test has been performed to investigate the dynamic tensile behavior of graphite. This type of test, which should be used for the mechanical characterization of brittle materials, is based on propagation and reflection of elastic waves: the fracture for spalling occurs when, in the material, the tensile stress state, obtained by the reflection on a free surface of a compressive pulse, exceeds the strength limit. These conditions are usually reached using a SHPB setup with a long bar specimen free at one end. Due to the low impedance and high damping of the graphite, the specimens are instrumented with strain-gages, in order to measure their strain histories, and a numerical approach is used to extract the material strength model parameters.

Introduction

In last decades, the interest for the investigation of strain-rate sensitivity of brittle materials became more and more widespread. In this sense, a lot of works can be found in literature, in which the mechanical behavior of ceramics like glass, graphite, concrete and rock-like materials was studied. Tests in compression are quite simple for this type of materials and results can be easily found in literature. On the contrary, obtaining data about strength and failure of material in a tensile state is a challenging task, especially because even small misalignments can lead to the failure of the specimen. To try to solve this problem different configurations, both in terms of specimen geometry and method of loading, were investigated, but results are strongly dependant of the test type and could have a low reproducibility.

All the previous considerations are even more difficult at high strain-rate loading conditions. However, if the material is used for dynamic applications, where the induced wave propagation becomes relevant, tensile loads can be generated from the reflection of compression waves on a free surface. This can happen in several applications, such as ballistic impacts, explosion or high energy deposition. This means that military, aerospace structural, civil protection and nuclear fields are involved in this kind of problem (e.g. [1, 2]).

Different methods were investigated, among which dynamic bending tests, Brazilian tests or perforation and penetration tests. In last decades, a lot of researchers suggested spalling test of long bars as one of the best ways to characterize dynamically brittle materials (see e.g. [3-6]).

This test is based on propagation and reflection of elastic waves in the specimen bar. Such conditions are usually reached using a Split Hopkinson Pressure Bar (SHPB) setup: a striker bar is launched against the input bar, which is in contact with a long specimen free at the opposite surface. The compressive pulse generated in the input bar is transmitted in the specimen and it is transformed in a tensile wave by the reflection on a free surface. This provokes the fracture for spalling, when the tensile stress state exceeds the strength limit. When failure occurs, at the fracture surface, part of the tensile wave is transmitted into the first fragment and part is reflected back in the other fragment.

In this work, the spalling test has been performed to investigate the dynamic tensile behavior of graphite. Due to the low impedance and the high damping of the graphite, the specimens are instrumented with strain-gages, in order to measure the strain histories transmitted in the first fragment. The low impedance of the graphite implies that it is not possible to evaluate the transmitted wave starting from the strain signals measured on the SHPB steel bars. Moreover, the high damping, proper of the graphite, produce a significant attenuation of the waves traveling in the specimen, making difficult the signals analysis. For these reasons, a numerical approach (developed by simulating the spalling test via the FE code AUTODYN [8]) is used to extract the material strength model parameters and the numerical results are compared with those obtained using a more classic analytical approach.

Material under investigation

Graphite R4550 used for the present experiment is a polycrystalline, isostatically pressed graphite produced by SGL Carbon [7], machined to obtain cylinders with 10 mm of radius and 200 mm of length. The nominal properties are reported in Table 1.

Table 1: Nominal Properties of R4550 Graphite from SGL Carbon datasheet [7].

Property (units)	
Average Grain Size (mm)	10
Bulk Density (g/cm^3)	1.83
Open Porosity (Vol%)	10
Pore size (mm)	1.5
Hardness (HR5-100)	95
Flexural Strength (MPa)	60
Compressive Strength (MPa)	125
Young's Modulus (GPa)	11.5
Thermal Conductivity (W/mK)	100

Experimental setup

The experimental equipment used for spalling tests is based on the use of a standard SHPB setup (see Fig. 1 for the scheme of the test). It consists of a gas gun 1.5 m long filled with compressed air. The striker and input bars are made in martensitic high-strength steel (14-4 PH) having a diameter of 10 mm. Two different strikers (100 and 80 mm long) are used in order to vary the amplitude and the length of the incident pulse. The striker velocity is measured by means of two photocells just before the impact. This allows controlling the amplitude of the compression pulse generated. The input bar is 3.4 m long, instrumented with a measuring point in the middle. The strain measurements are performed by means of half-bridge semiconductor strain-gages (KYOWA KSP-1-350-E). The Wheatstone bridge was completed with standard resistors and the output signals were recorded with a National Instrument PCI-express DAQ (8 channels, 14 bit, 3 MHz simultaneous sampling).

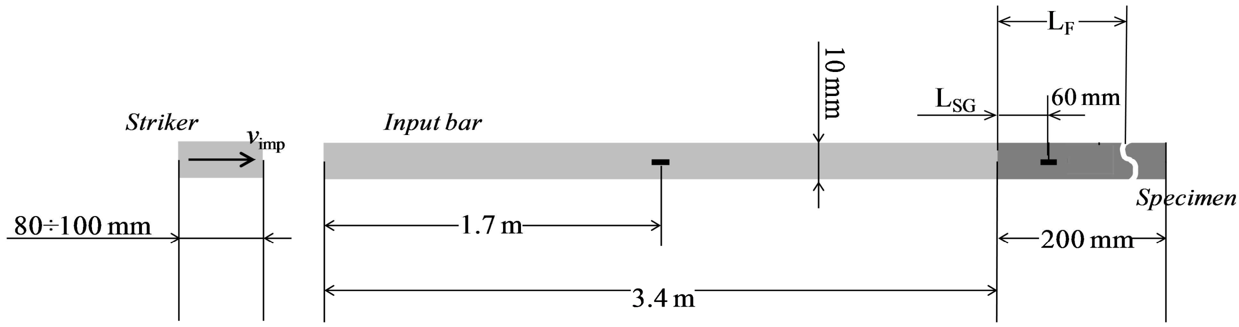

Fig. 1: Scheme of the experimental test.

The specimens are bars in contact with the input bar at one extremity and free at the other one (see Fig. 1). The strain in the specimen is measured by half-bridge standard resistive strain-gages (HBM). The strain-gages used have a nominal resistance of 350 Ω with a nominal gage factor of 1.93. In both cases, the supply voltage is 10 V.

The strain in the specimen bar is measured at 60 mm from the surface impacted by the input bar (see Fig. 1): the position is decided to be sure that, for each test, the fracture is situated at higher longitudinal coordinates. The wave which travels backwards through the first specimen fragment is limited in amplitude by the tensile strength of the material. This means that it has no more chances to generate another fracture surface (supposing that there are no inhomogeneities inside the material). On the other hand, the wave transmitted back into the second fragment could exceed the tensile strength of the material and create a new fracture surface. Ideally, this process occurs in the fragment closest to the free edge of the specimen until the amplitude of the wave becomes lower than the tensile strength of material.

Each test is recorded with a high-speed camera with an acquisition rate of 20000 frames per second, to control the evolution of the test. Some preliminary tests are performed, in which the impact velocity is so low that no macroscopic failure occurs in the specimen.

Table 2: List of all the experimental tests performed.

TestID	L_{SG} (mm)	Failure	L_F (mm)
gr_1a	60.1	no	-
gr_1	60.1	yes	146.0
gr_2	60.3	yes	129.7
gr_3	62.4	yes	146.4
gr_4	59.8	yes	152.5
gr_5a	60.0	no	-
gr_5	60.0	yes	121.0
gr_6	60.0	no	126.0

In Table 2 is reported the list of all the experimental tests performed together with the identification name of the test, the position of the strain-gages, whether the specimen fails or not during the test and finally, in the former case, the fracture lengths from the impacted base of the cylindrical specimen (see Fig. 1). The specimens used for the preliminary tests (no failure) are then used for the next test inducing the failure (same ID number followed by the letter b). As can be noticed from the results reported in Table 2, the fracture surface is always situated after the strain-gage, as expected. In this way, after the fracture, it is sure that the strain-gage continues to measure the part of the wave, which remains trapped in the first fragment of material.

Experimental data analysis procedure

The approach for the analytical elaboration of the experimental data is described below. The authors want to remark that this is an approximate procedure, from which it is possible to obtain an estimation of the strain at failure.

As it is well known, in graphite the wave dispersion, as well as the material damping, are phenomena which have to be taken into account. As a matter of fact, in case of wave propagation inside the material, these two effects produce a significant modification of the wave profile. The problem is especially related to the fact that the strain measuring points (strain-gages positions) are not placed where the fracture occurs. So, it is necessary to properly correct the signal measured by the strain-gage, in order to go back to the fracture point.

In this work the superposition of wave dispersion and material damping is estimated fitting the experimental data obtained from the tests in which no failure occurs.

The starting point of the analysis is the signal, expressed in Volts, directly acquired at the ends of the Wheatstone bridge. Voltage signals are then transformed into strain signals and reset to have a zero mean value. The signals are positive in tension and negative in compression. In Fig. 2, the experimental data in terms of strain vs. time curves for one specimen is reported both in the cases with and without failure (gr1a and gr1c in reference to Table 2).

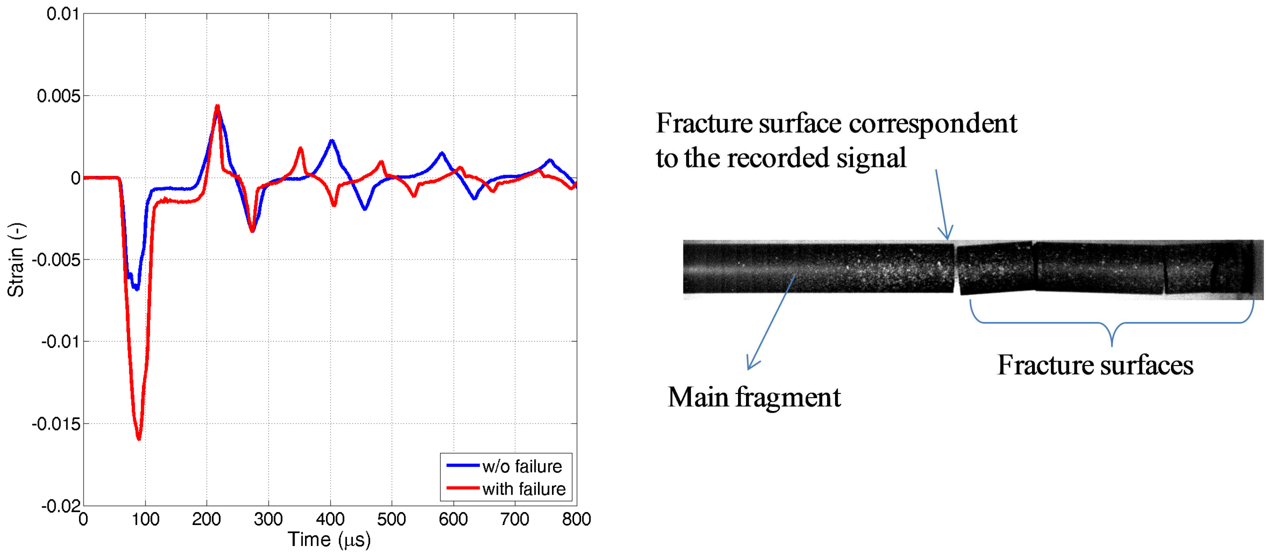

Fig. 2: Experimental data for graphite: comparison between the signal in case with and without failure (left); image taken by the high speed camera during the test (right).

In Fig. 2, a picture recorded by the high speed camera is also reported and some observations can be done. Qualitatively analyzing the results it is possible to notice that, when the fracture occurs, the signal is abruptly interrupted; after that the distance between the peaks changes, since the measured signal corresponds to the part of the wave trapped in the main fragment. Another point is the fact that, after the end of the compressive wave, the signal does not return to zero: this will be further investigated in the future, but as it will be presented in the next paragraphs, the visco-elastic behavior of graphite could be partially responsible for this effect.

Sound speed estimation. In the spalling test the specimen is subjected to a uniaxial stress state: in this condition the longitudinal stress/strain waves travel inside the specimen with a phase velocity equal to the sound speed $\left(C_0 = \sqrt{E/\rho} \right)$ of the material at a frequency equal to zero [9]. The first step of the procedure implies the determination of this speed. First of all, each specimen is measured and weighted and the density is calculated. Then, an average value is considered on the basis of all the available data: 1853.7 kg/m^3 is the obtained value for density.

Before describing the procedure used for the estimation of the sound speed, it is necessary to notice that, also for the cases in which failure does not occur, the sound speed increases during the test. As a matter of fact, the time distance between two successive peaks decreases; this could be, in general, correlated to a non-linear behavior of the material: increasing strain amplitudes, the mechanical response deviates more and more from the linearity, decreasing the slope and consequently decreasing the speed of propagation. From this, the decision to evaluate the trend of the sound speed as a function of the distance covered by the wave. The evaluation is performed for each specimen in which the failure occurred and is based on the measurements reported in Table 2 (positions of strain-gages and fracture surface). In more details, excluding the first peak in compression, the two successive peaks in compression and the first three peaks in tension are considered. By calculating the differences in time and space between each couple of peaks, it is possible to obtain the diagram of Fig. 3 (left), in which the calculated sound speeds (circle markers) are reported as a function of the total length travelled by the wave. The zero is set in the position of the strain-gage (L_{SG}). The experimental data are then fit with an appropriate function (solid line), which allows, once the distance between the strain-gage and the fracture surface is know, to obtain the value of the sound speed in correspondence with the fracture length (star marker).

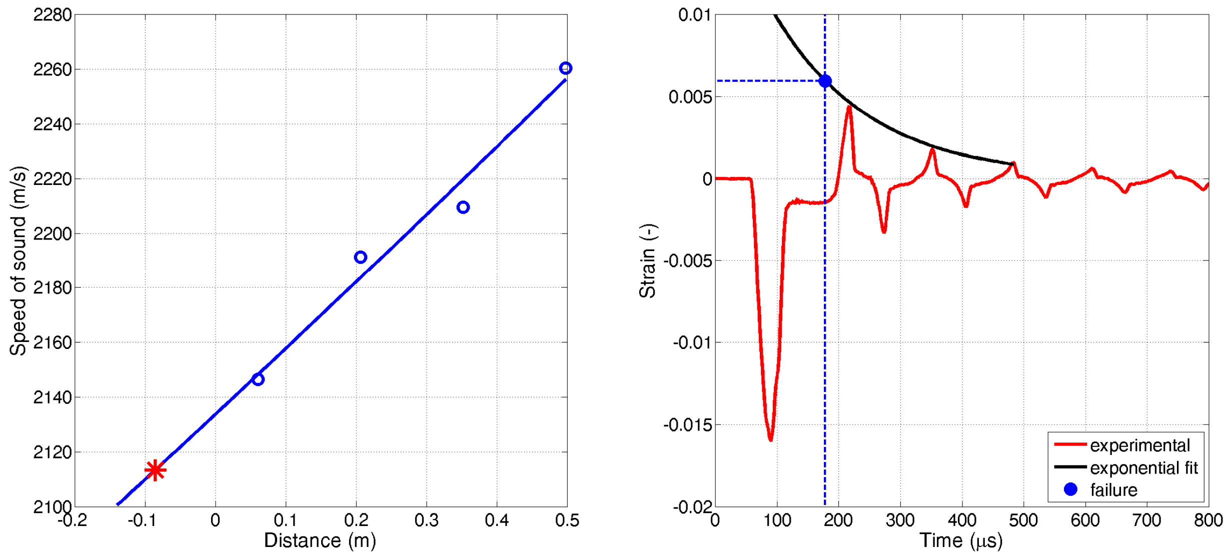

Fig. 3: Evaluation of the trend of the sound speed and identification of trend as a function of the total length covered by the wave (left); wave dispersion and material damping estimation using an exponential function to fit the data and identification of the strain to failure (rigth).

Wave dispersion and material damping. As anticipated before, the effects of these two phenomena, which are quite significant for graphite, are considered together. To do this, the maxima (tension) are fitted with an exponential law ($\varepsilon = Ae^{-Bt}$), as reported in Fig. 3 (right). This interpolation is performed for each test, in order to extract the coefficients A_i and B_i, which allow reconstructing the decrement of the maxima in each test with failure.

Failure estimation. The fracture occurs when the reflected tensile wave amplitude reaches the material strength: the wave starts to propagate backwards along the sample with reduced amplitude generating the first positive signal recorded by the strain-gage. In any case, due to the fact that the wave traveling through the specimen changes both in shape and in amplitude, the measured maximum value is not exactly the tensile strength of the material, which, instead, is greater than this value. To get the correct value, it is necessary to know the wave amplitude damping between the fracture surface and the strain-gage position, given by the time passed between the strain-gage recording and the fracture. This can be easily evaluated from the distance between strain-gage and fracture surface and the sound speed at fracture. Once the time in which the fracture occurs is known, using the exponential fit, it is possible to evaluate the strain at failure (see Fig. 3, right). The results obtained in terms of strain to failure from all the tests are averaged and a mean value of 0.006 is found.

Numerical model

As mentioned before, the analytical method used for the signal processing is approximated. As a refinement, a numerical approach is followed based on FE model, solved in Autodyn © V14.5 [8].
From the consideration done in the previous paragraph, it is clear how the commonly used elastic models for graphite cannot correctly describe the wave propagation, due to the lack of an energy dissipating component. As a matter of fact, given that graphite shows a non-linear behavior and due to damping and dispersion effects which modify the shape of the wave, a visco-elastic strength model should be used.
The proposed model divides the total stress tensor in two parts: an elastic stress tensor and a deviatoric visco-elastic stress tensor, which correspond, respectively, to the energy conservative part and the energy dissipative part. The elastic part is correlated to the Bulk modulus (B) and the long term shear modulus (G_∞). The dissipative part expresses the shear modulus as a relaxation function, defined as:

$$G(t) = (G_0 - G_\infty)e^{-\beta t}$$

where G_0 is the instantaneous shear modulus and β the decay constant. The failure model used for simulating material fracture is based on the maximum strain and assigned only to the elements situated in correspondence with the position of the fracture.
The graphite sample is modeled using a 2D axis-symmetric geometry, loaded by a trapezoidal velocity profile imposed as a boundary condition on the impacted surface. No other boundaries are applied to the body, which is free to move after the impact.
A reverse engineering approach is used in order to obtain, at the same time, the parameters of both the strength and the failure models, based on the experimental data in which the failure occurs. From the analysis is excluded the first peak in compression, which is correlated to the specimen before the fracture. The parameters, obtained for the test labeled as gr_2, are reported in Table 3.

Table 3: Material model parameters for strength and failure models.

Property (Units)	**Value**
Density (kg/dm^3)	1.85
Bulk modulus (GPa)	3.33
Instantaneous shear modulus (GPa)	4.26
Long term shear modulus (GPa)	3.04
Visco-elastic decay constant (ms^{-1})	40
Principal tensile strain at failure (-)	0.0051

The result obtained from the numerical simulation in term of longitudinal strain vs. time curve is reported in Fig. 4. The time history is referred to the longitudinal position of the strain-gage and this allows comparing the curve with the experimental data. The comparison is made starting from the end of the first compressive pulse.

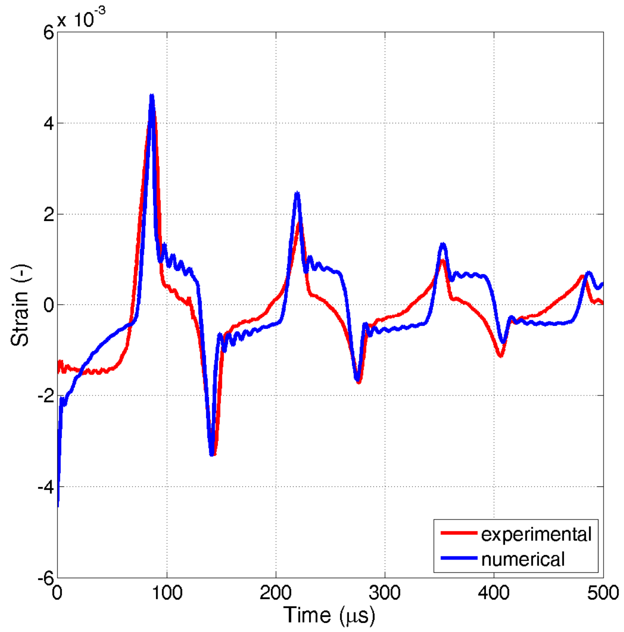

Fig. 4: Longitudinal strain vs. time curve: comparison between numerical and experimental results.

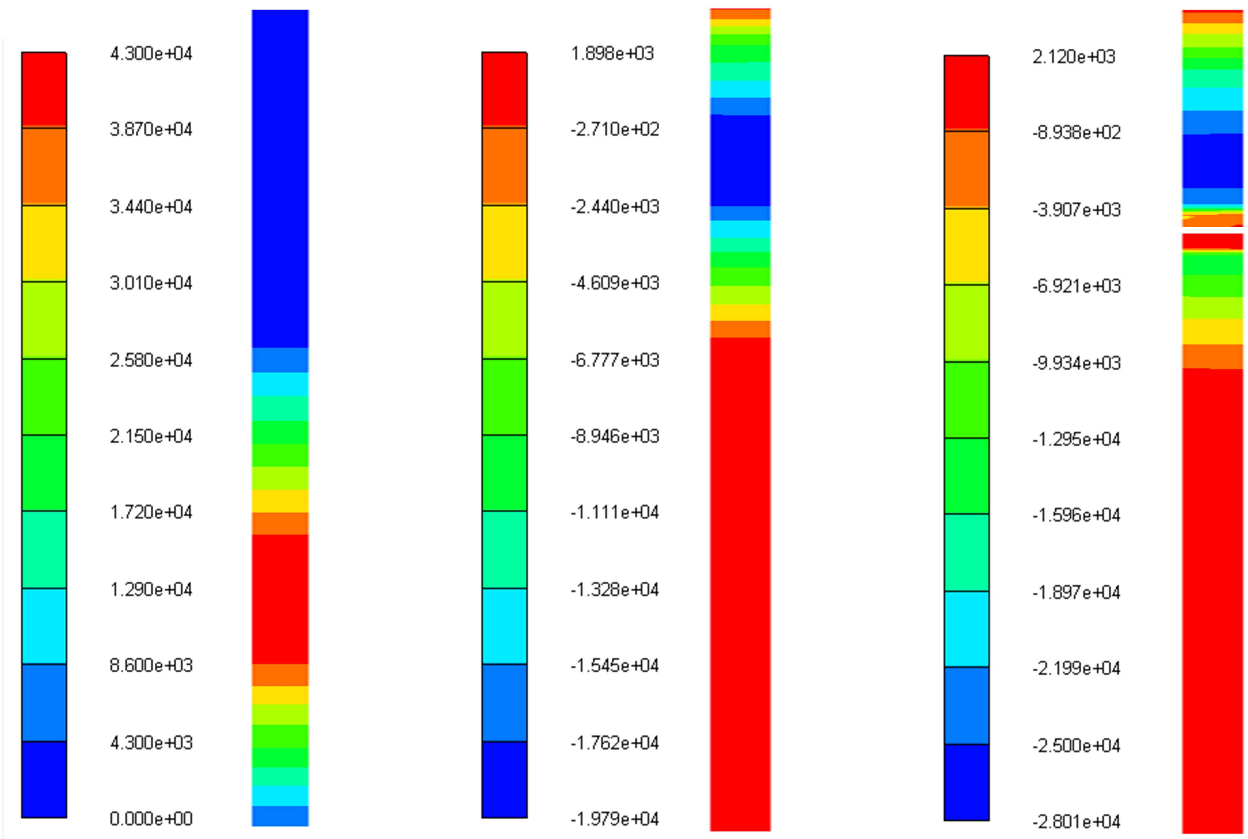

Fig. 5: Sequence of the pressure wave propagation.

As it can be noticed, the visco-elastic model is able to reproduce the time decay of the amplitude of the strain signal as well as the speed of propagation of the signal itself with a reasonable level of accuracy. Moreover, as anticipated before, also in the numerical model there is the presence of residual compression or tension after the end of the signal.
In Fig. 5 the sequence of the pressure wave propagation inside the graphite bar is reported at three different time steps: the compressive wave travels along the bar and once it reaches the free surface it is reflected back as a tensile wave. When the overlap of compressive and tensile wave ends, the graphite fails producing the fracture surface.

Conclusions

In this work, the spalling test was performed to investigate the dynamic tensile behavior of graphite. The experimental data were analyzed to get the value of stain to fracture of the material. As first approximation, the data were elaborated with an analytical procedure, which, assuming the material to be elastic, estimates the strain to fracture, treating the problems of dispersion and damping in a simplified manner: the damping in graphite is quite significant and makes difficult the data processing. In order to try to improve the quality of the data analysis, a numerical model was developed in Autodyn using a 2D axis-symmetric approach. The material behavior was reproduced with a visco-elastic model and the material parameters were varied in order to obtain a good approximation of the experimental data. Nevertheless the model is quite simple, it allowed to reproduce, with a sufficient level of accuracy, the dynamic of the wave propagation and in particular the attenuation due to the internal damping of the material. The graphite showed, especially at high deformation, a non-linear behavior, so the model could be further improved, although it is a good compromise for the modeling of graphite subjected to impulsive loads.

References

[1] H. Kim, Y.S. Lee, D.H. Kim, N.S. Park, J. Suh, J. O. Kim, S.I. Moon, Evaluation thermal shock strengths for graphite materials using a laser irradiation method, J. Mat. Sci. Eng. A 387-389 (2004), DOI:10.1016/j.msea.2004.01.136.

[2] A. Kurumada, T. Oku, H. Harada, K. Kawamata, S. Sato, T. Hiraoka, Effects of burn-off on thermal shock resistances of nuclear carbon materials, Carbon Vol. 35 N. 9 pp. 1157-1165, 1997, PII:S0008-6223(97)00088-2.

[3] J. Najar , Dynamic tensile fracture phenomena at wave propagation in ceramic bars, J Phys IV, Colloque C8 Supplement au Journal de Physique III, No. 4, 1994; 647–52.

[4] M. Diamaruya, H. Kobayashi, T. Nonaka, Impact tensile strength and fracture of concrete, J Phys IV, Colloque C3 Supplement au Journal de Physique III, No. 7, 1997; 253–8.

[5] F. Galvez Diaz-Rubio, J. Rodriguez, V. Sanchez-Galvez, Tensile strength measurements of ceramic materials at high rates of strain, J Phys IV, Colloque C3 Supplement au Journal de Physique III, No. 7, 1997; 151–6.

[6] C. Johnstone, C. Ruiz, Dynamic testing of ceramics under tensile stress, Int. J. Solids. Struct. 1995; 32(17/18):2647–56.

[7] SGL CARBON GmbH Catalogue: SGL Carbon's Graphite Specialties, Materials and Production for Continuous Casting Technology, http://www.skckarbon.com.tr/UserFiles/Image/endustriyel/sdimvu.pdf.

[8] ANSYS AUTODYN User's Manual – Release 2010, ANSYS Inc. (2010).

[9] Weinong Chen, Bo Song, Split Hopkinson (Kolsky) Bar Design, Testing and Applications, Mechanical Engineering Series, ISBN 978-1-4419-7981-0, Springer (2011).